Electrical Power Quality and Utilisation, Journal Vol. XIV, No. 2, 2008

Distributed System for Power Quality Improvement

Ryszard KLEMPKA

AGH-University of Science and Technology, Krakow POLAND

***Summary*: On the basis of the current trends for solving complex technical problems, a new concept of power quality improvement is proposed. It consists in creating a distributed system for supply conditions improvement in a given islanding power system, in e.g. geographical terms (with determined points of delivery), or as an internal installation system of an industrial consumer.**

Key words:
distributed system, power quality, genetic algorithms

1. INTRODUCTION

On the basis of observation of the current trends for solving complex technical problems, the author proposes a new concept of power quality improvement. It consists in creating a distributed system for supply conditions improvement in a given self contained power system in the geographical sense (an autonomous or islanding power system with determined points of delivery), or an industrial consumer internal installation.

A power system includes various distributed consumers that *adversely impact* the power quality indices. In the same system there are many disturbance-sensitive loads. Limit values of power quality indices (compatibility levels) are set for the whole system. The power system comprises also various distributed controlled devices intended for power quality improvement, i.e. controlled sources of reactive power (static compensators, not fully loaded synchronous motors with excitation current control), dynamic voltage restorers, active filters and distributed power sources. There is also other equipment dedicated for specific use, which, if designed for such purposes, may perform the function of the fundamental component reactive power compensators, voltage stabilizers, and high-order harmonics parallel active filters. A specific role can be played by adjustable speed drives (ASD) which, being common loads in industrial installations, are of particular significance for the power quality improvement. Most ASD drives incorporate an input a VSI inverter, which guarantees sinusoidal input current in all modes of motor operation, and apart of generation of the current necessary to supply the active power required by mechanical load, is capable (if adequately oversized) of generating an additional current component according to the reference generated by a central control system intended for compensation of other parallel disturbing loads (Fig. 1.1).

According to the presented concept, the objective of this work is to develop a central control system which, on the basis of the set of input signals (mainly voltages and currents measured at selected points of a power system), will generate reference signals for several distributed controlled devices to be jointly used for the supply quality improvement. The following devices to be controlled from the central control system shall be taken into consideration in the first place:

a) SVC compensators – TSC or TCR/FC
b) synchronous motors with excitation current control
c) distributed power sources (photovoltaic systems, wind turbine generators with indirect frequency converters, etc.)
d) parallel active power filters (APF) and/or adjustable speed drives (VSI type).

An example power system with schematic diagram shown in Figure 1.2 will be discussed below. The system comprises

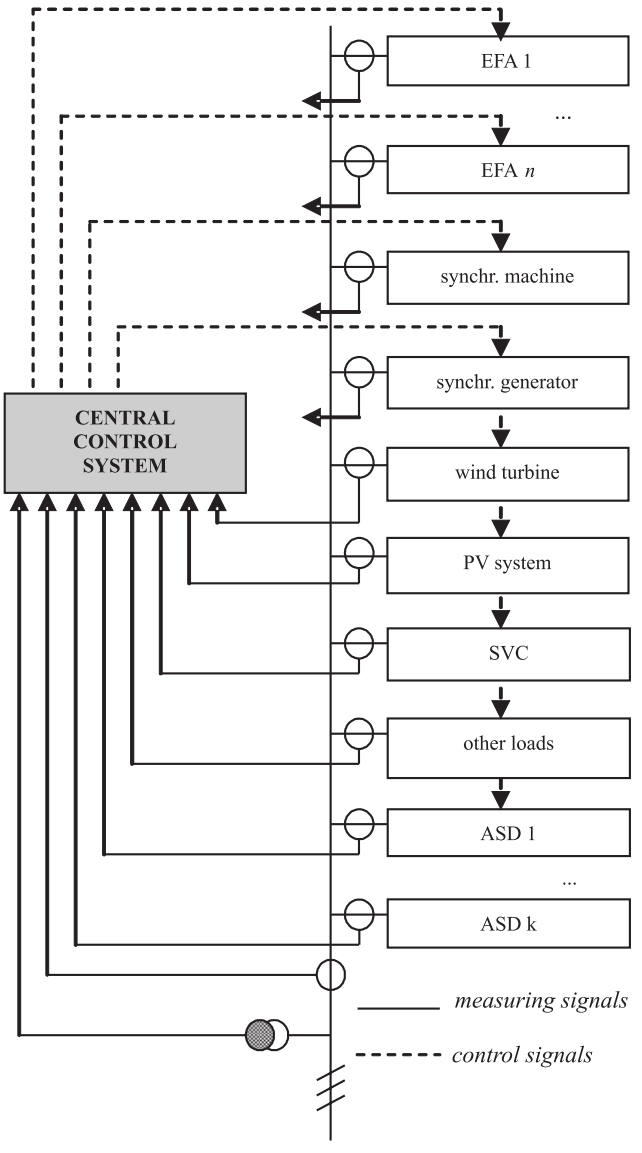

Fig. 1.1. The concept of a distributed system for power quality improvement

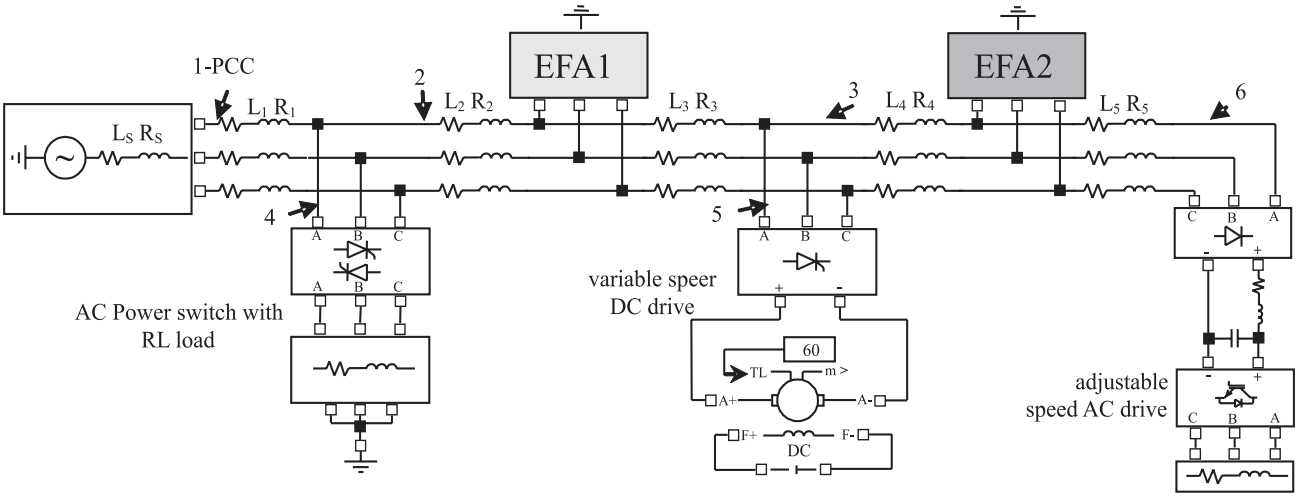

Fig. 1.2. An example power system

non-linear loads, which the source of voltage and current distortion in the system's nodes.

The example power system shown in Figure 1.2 contains three non-linear loads, which consume reactive power and generate harmonics [6, 7, 8, 9, 10]. Current sources — shunt active filters — are connected in the system's selected nodes. Their purpose is reduction of the voltage distortion level at PCC and power factor control in the installation. In industrial applications the role of active power filters can be played by adjustable speed drives with indirect frequency converters which, if are not fully loaded or are designed to be properly oversized, can also function as active parallel compensators. Due to various options of optimization, the power of active filters has not been determined in this work. The optimization was carried out with the first filter maximum current limitation at various levels, as well as without the limitation.

In most publications, attempts at solution of the presented problem were based on the analytical solution of the circuit (this requires its complete identification, which normally is impracticable) or, with a larger number of compensating devices, on the theory of multi-agent systems. [14, 16]. In this paper genetic algorithms were employed to solve the formulated multi-criterial optimization task in accordance with the presented conception.

An example of the current waveform at PCC — the system point (1), is shown in Figure 1.3, and figure 1.4 shows the voltage at PCC and its spectrum. As can be seen from figures, the waveforms are distorted. Figure 1.5 shows the load currents at points 4, 5 and 6, respectively.

The basic parameters are: $THD_u = 8.19\%$, $THD_I = 22.81\%$ and phase shift of the voltage and current fundamental harmonics $\varphi_{(1)} = 27.85°$. In further considerations the factor M was taken as the measure of additional losses associated with reactive component of the current fundamental harmonic and harmonic currents. The factor M defined by relation:

$$M = 1000 \cdot \left\{ \left(I^2_{RMS(\text{pkt2})} - I^2_{(1)cz(\text{pkt2})} \right) R_2 + \right.$$
$$\left. + \left(I^2_{RMS(\text{pkt3})} - I^2_{(1)cz(\text{pkt3})} \right) R_3 \right\} = 1.07 \tag{1.1}$$

Though it is not directly related to power losses in the system as expressed in absolute units, it is a useful measure of adverse effects of undesired current components.

The form of this relation results also from practical reasons, i.e. minimization of the number of measurement points in the system.

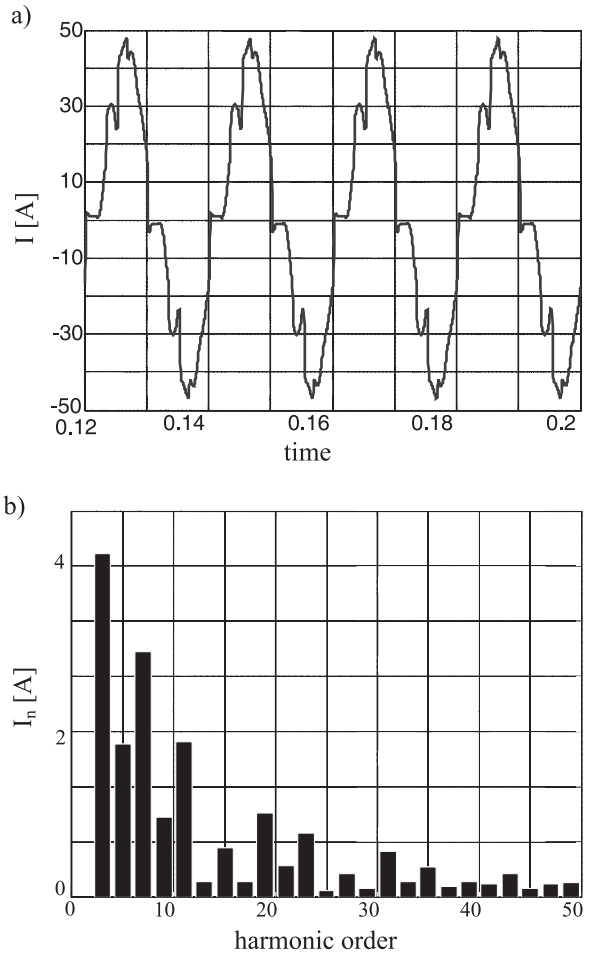

Fig. 1.3. The current (a) and its spectrum (b) at PCC (1))

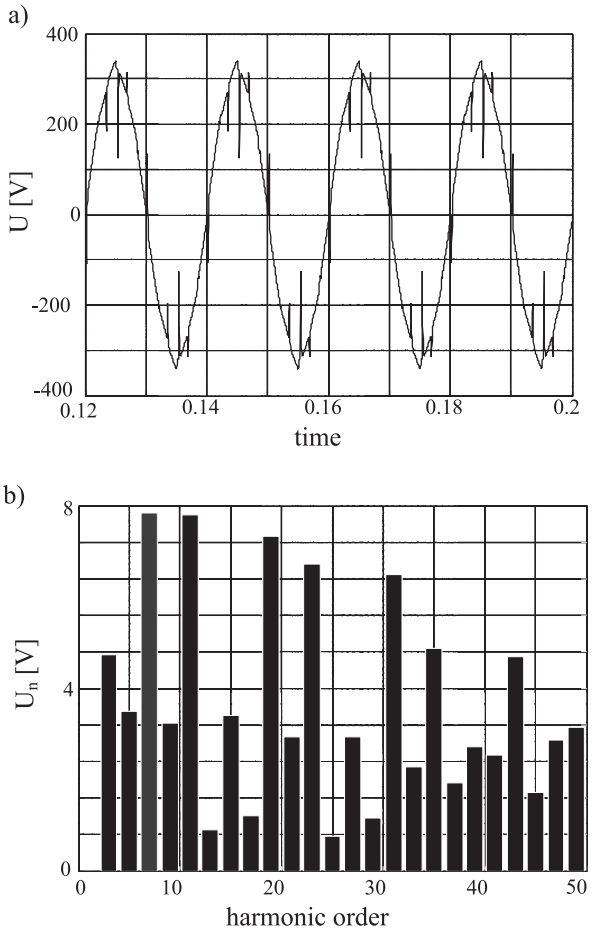

Fig. 1.4. The voltage (a) and its spectrum (b) at PCC (1)

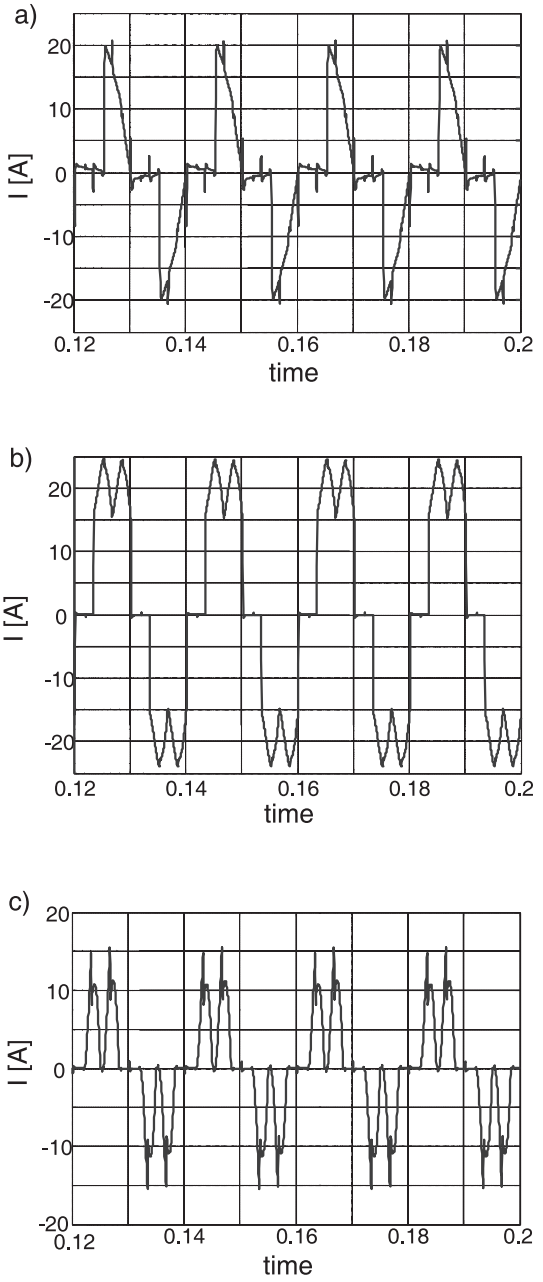

Fig. 1.5. Steady-state current waveforms in selected phase of discussed loads (Fig. 1.2) for selected operating conditions at points 4 (a), 5 (b) and 6 (c)

2. REACTIVE POWER COMPENSATION

Further in this work are presented simulation effects of the central control system operation, which reduces various objective functions values, independently or in their combinations e.g.: reactive power compensation, reduction of system losses, reduction of voltage and current distortion, etc. This subsection deals with the phase shift between the voltage and current fundamental harmonics. This goal will be attained in four consecutive stages.

2.1. Reduction of the phase shift

The first stage is exclusively the minimization of the phase shift between the voltage and current fundamental harmonics at PCC (point 1), i.e. reactive power compensation.

The objective function of the Genetic Algorithm, defined for this purpose has the form:

$$f_{goal} = \begin{cases} 10^{10} * |\varphi - 2| & for \ \ \varphi < 2^\circ \\ \varphi - 2 & for \ \ \varphi \geq 2^\circ \end{cases} \qquad (2.1)$$

Bearing in mind that the Genetic Algorithm is a random algorithm, i.e. it is possible that the Genetic Algorithm solutions will overcompensate the system, the optimization goal is to achieve an arbitrary assumed phase-shift value not less than $\varphi(1) = 2°$. The objective function will "punish" solutions with smaller values by assigning them vary large value of the objective function (arbitrary chosen weight of 10^{10}).

Figure 2.1 shows values of the voltage (a) and current (b) fundamental harmonic during the central controller search for the optimal solution. During the optimization the value of the voltage fundamental harmonic increases whereas the value of the current fundamental harmonic decreases. Figure 2.1c shows the phase-shift between the voltage and current fundamental harmonics, and figure 2.1d shows the factor M value. The phase shift decreased, as assumed, to 2°, whereas the factor M increased from 1.07 to 5.7. Figures 2.1e and 2.1f show values of both active fitters currents (here the term "active filter" refers to a device, which apart of filtering, can also be a source of the fundamental harmonic reactive current). It should be noted that the objective function does not influence the current distribution between them; it is a

random distribution. Changes in total harmonic distortion factors THD_u and THD_i are shown in Figures 2.1g and 2.1h, respectively. Since the voltage fundamental harmonic value increases, THD_u factor decreases, and conversely, due to reduction of the current fundamental harmonic value, THD_i factor increases.

The spectra of voltage and current at PCC, after the central control optimization in order to minimize the system reactive power, are shown in Figures 2.1i and 2.1j. These spectra show no changes as compared to the situation prior to the filters connection.

As shown in Table 2.1, Genetic Algorithm has already completed optimization of the active filters control and, therefore, minimized the system reactive power. The currents of both filters are tabulated in the complex form (subscript "cz" denotes the real component, subscript "b" denotes the imaginary component).This optimization is of random nature with respect to the power generated by filters to the system.

2.2. Reduction of the phase shift and power losses

In order to avoid the randomness of power distribution between the filters, the expression for the objective function has been altered to account for system losses at two selected points (2, 3). Taking the losses into account will influence the distribution of power generated by filters to the system.

Thus the objective function takes the form:

$$f_{goal} = \begin{cases} 10^{10} \cdot |\varphi - 2| & for \ \ \varphi < 2° \\ 3 \cdot |\varphi - 2| + 20000 \cdot M & for \ \ \varphi \geq 2^c \end{cases} \qquad (2.2)$$

Results of the optimization performed for such defined objective function are depicted with graphs in Figure 2.2.

Figure 2.2 shows fundamental harmonics of the voltage (a) and current (b) during the optimization. Figure 2.2c shows changes in the phase shift between the voltage and current fundamental harmonics. The phase angle attains the assumed value of 2°. The characteristic 2.2d shows the factor M that represents power losses in the system. As can be seen from Figure, the value of factor M has decreased form 1.07 to 0.2452, i.e. to 22.92% of its initial value. The active filters currents are shown in Figures 2.2e and 2.2f. Their values are determined by the Genetic Algorithm so as to minimize the factor M. Distortion factors THD_u and THD_i are shown in Figures 2.2g and 2.2h, respectively.

Values of active filters currents are given in table 2.2.

Table 2.1. The currents of active filters (complex components)

n	$I_{Re(EFA1)}$	$I_{Im(EFA1)}$	$I_{Re(EFA2)}$	$I_{Im(EFA2)}$
1	0	–0.78	0	–11.86

Table 2.2. The complex components of active filters currents

n	$I_{Re(FA1)}$	$I_{Im(FA1)}$	$I_{Re(FA2)}$	$I_{Im(FA2)}$
1	0	–11.91	0	–0.53

2.3. Reduction of the phase shift, power losses and operating costs

Further modification to the Genetic Algorithm accounts for the active filters operating costs. Operating costs of these devices consist of two components: activation cost and costs proportional to the filter current. Assuming the activation cost of the first filter is *a* times greater than the activation cost of the second filter, and a unit cost per ampere of the first filter current is *b* times greater than that of the second filter, the objective function of the Genetic Algorithm takes the form:

$$f_{goal} = \begin{cases} 10^{10} \cdot |\varphi - 2| & for \ \ \varphi < 2° \\ 3 \cdot |\varphi - 2| + 20000 \cdot M + K & for \ \ \varphi \geq 2^c \end{cases} \qquad (2.3)$$

$$K = a \cdot (I_1 \neq 0) + 1 \cdot (I_2 \neq 0) + b_1 \cdot I_1 + b_2 \cdot I \qquad (2.4)$$

According to the above assumptions the factor *K* depends on operating costs of both active filters and it is accounted for in the objective function. Optimization of the central control was performed for the control principle formulated as above and the coefficients a, b_1 and b_2 assumed 2, 0.33 and 0.1, respectively. The results are shown in Figure 2.3.

Figure 2.3 shows fundamental harmonics of the voltage (a) and current (b). Their graphs are similar to those obtained in former optimizations. Figure 2.3c shows changes in the phase shift between the voltage and current fundamental harmonics during the optimization. The phase angle attains the value of 2°. The factor M is shown in Figure 2.3d. Its value decreases form 1.07 to 0.37 what makes 33.6% of the initial value. In this optimization the factor M has not decreased to as small a value as in the former case. Taking into account the operating costs of active filters affects the solution quality. Figures 2.3e and 2.3f show the currents of active filters. Since the operating costs of the first filter are higher, the Genetic Algorithm has "decided" to reduce its contribution as compared to the former optimization, whereas the second filter current contribution to the task of power quality improvement, has increased. Distortion factors THD_u and THD_i are shown in Figures 2.3g and 2.3h, respectively. Their behavior is similar to that in former optimizations.

Values of active filters currents are given in Table 2.3.

2.4. Reduction of the phase shift, power losses and operating costs with limitation of maximum current

Maximum output current of a real current source, employed for power quality improvement, is limited. Hence, in the next optimization it was assumed that the maximum output current of the first filter must not exceed 6A.

The central control optimization was performed for the same objective function as in subsection 2.3, and with limit imposed on the maximum output current of the first filter, the results are presented in Figure 2.4.

Figure 2.4 shows fundamental harmonics of the voltage (a) and current (b) at PCC. In all optimizations amplitudes values of these harmonics followed similar pattern. Figure 2.4c shows the phase shift between the voltage and current

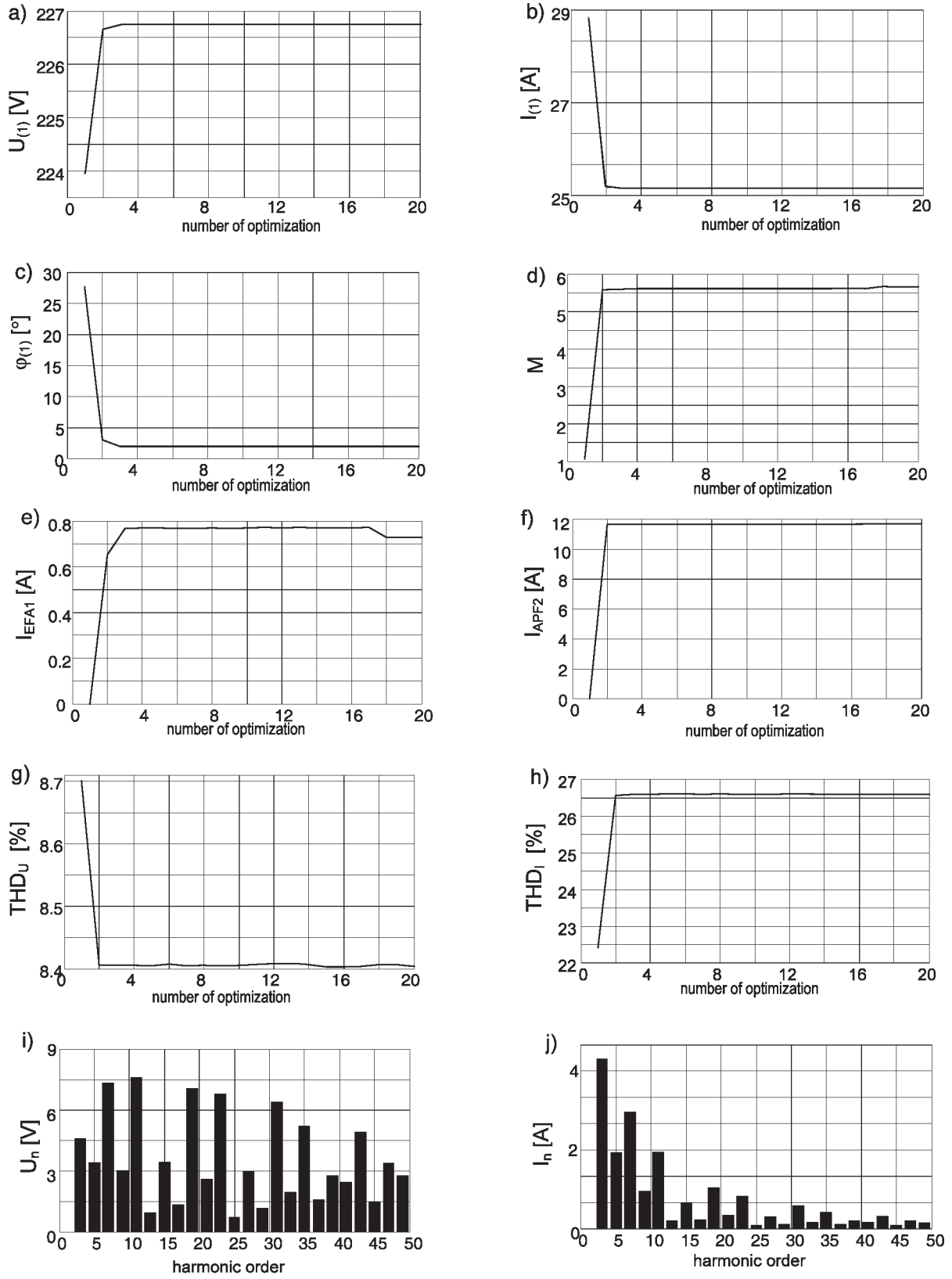

Fig. 2.1. Values of the voltage (a) and current (b) fundamental harmonics; phase shift $\varphi_{(1)}$ (c); factor M (d); currents of active filters EFA1 (e) and EFA2 (f); distortion factors THD_u (g) and THD_i (h) during the optimization; spectra of the voltage (i) and current (j) after minimization of the system reactive power

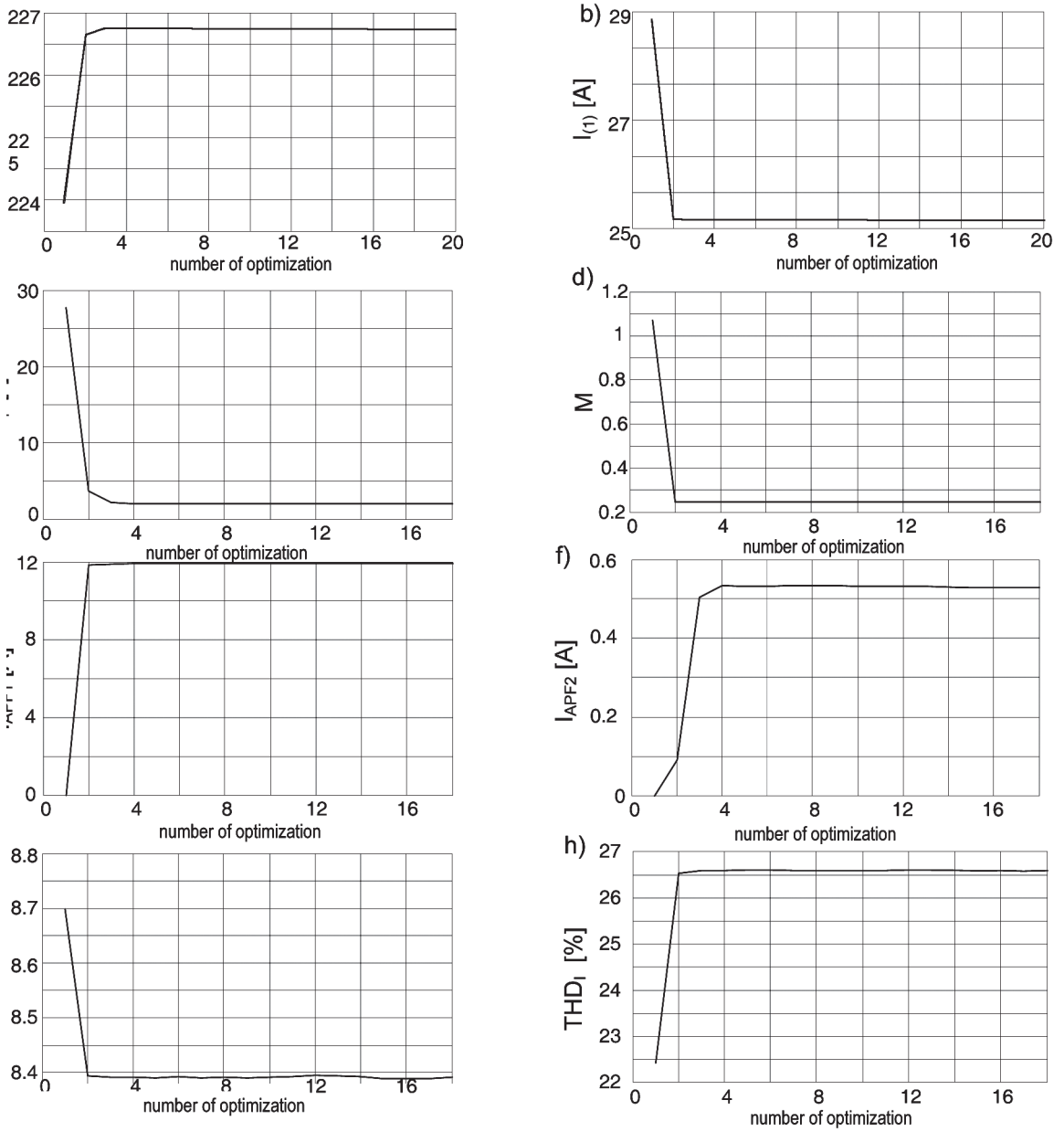

Fig. 2.2. Fundamental harmonics of the voltage (a) and current (b); phase shift $\varphi_{(1)}$ (c); the factor M (d); currents of active filters (e) and (f); distortion factors THD_u (g) and THD_i (h)

fundamental harmonics. The phase shift after optimization is ca. 4°. In this case the expected value of two degrees has not been reached. The factor M decreases form 1.07 to 0.85 what makes ca. 80% of the initial value. This value is smaller than the initial one, however, a weaker influence of the factor M on the optimization is observed after limitation of the active filter maximum output current. The currents of active filters are shown in Figures 2.4e, 2.4f and in Table 2.4. Limitation of the active filter output current to 6A is evident. Distortion factors THD_u and THD_i are shown in Figures 2.4g and 2.4h, respectively.

Table 2.3. Components of the active filters currents

n	$I_{Re(FA1)}$	$I_{Im(FA1)}$	$I_{Re(FA2)}$	$I_{Im(FA2)}$
1	0	–9.34	0	–3.1

3. REACTIVE POWER COMPENSATION AND HARMONICS REDUCTION AT PCC

It has been demonstrated that central control employing a Genetic Algorithm for the purpose of power quality improvement is feasible. The presented optimizations take into account only the reactive power compensation in a system. In practical applications there is often a necessity for voltage harmonics mitigation at PCC. Therefore in further examples the reactive power compensation will be carried out simultaneously together with elimination of six subsequent odd harmonics: 3, 5, 7, 9, 11 and 13.

3.1. Reduction of the phase shift and harmonics reduction

The objective function of Genetic Algorithm consists of two parts. The first one (3.1a) is related to optimization in the domain of fundamental harmonic, i.e. reactive power

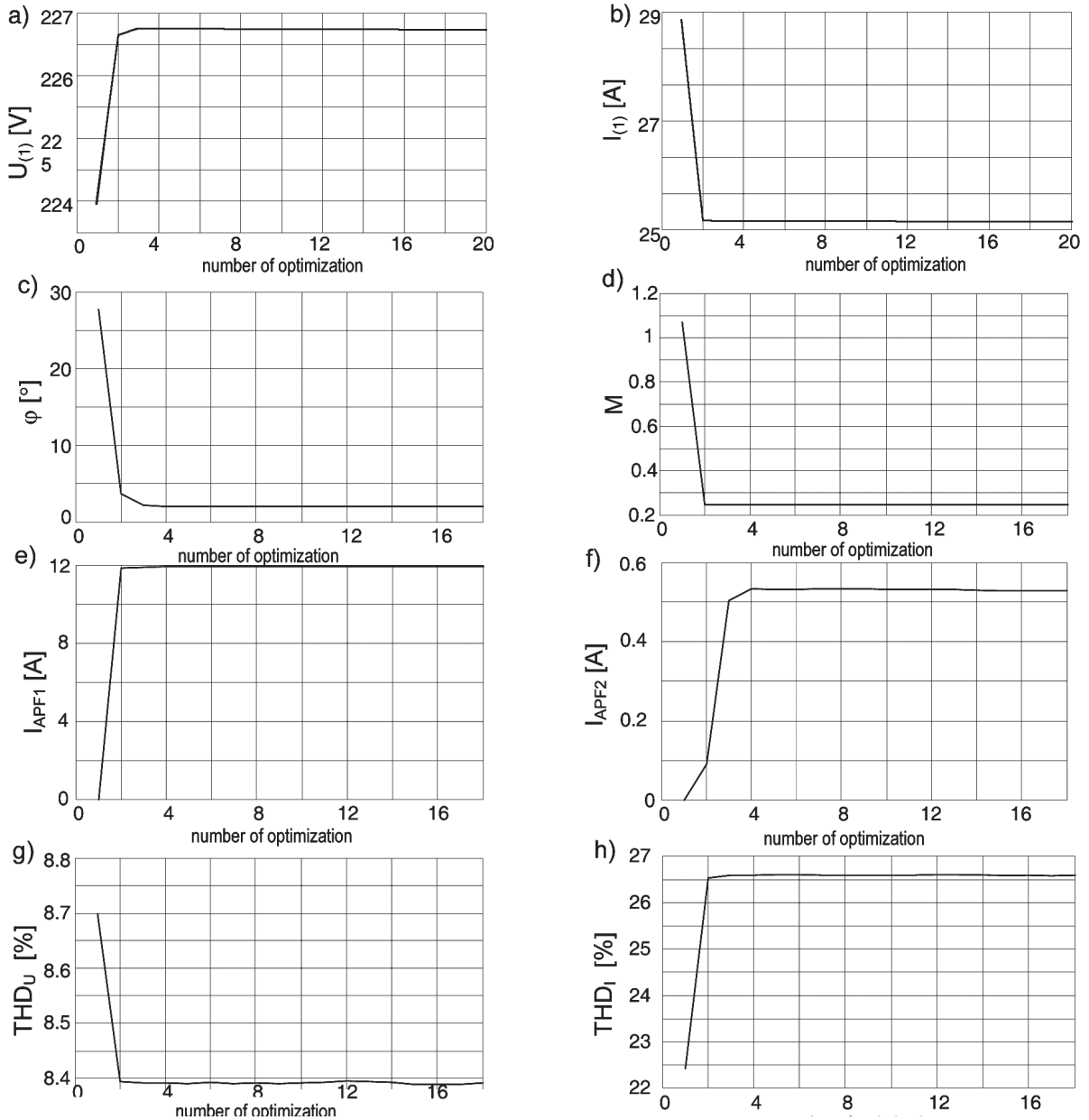

Fig. 2.3. Fundamental harmonics of the voltage (a) and current (b); phase shift between the voltage and current fundamental harmonics (c); the factor M (d); rms values of the active filters currents (e and f); distortion factors THD_u (g) and THD_i (h)

compensation, the second part (3.1b) is associated with minimization of harmonics:

$$f_{goal} = \begin{cases} 10^{10} * |\varphi - 2| & for \ \ \varphi < 2^\circ \\ \varphi - 2 & for \ \ \varphi \geq 2^\circ \end{cases} \tag{3.1a}$$

$$f_{goal} = U_h \tag{3.1b}$$

Table 2.4. Components of the active filters currents

n	$I_{Re(FA1)}$	$I_{Im(FA1)}$	$I_{Re(FA2)}$	$I_{Im(FA2)}$
1	0	–6	0	–5.5

Figure 3.1 shows the investigation results for the objective function 3.1. The minimized voltage (c) and current (d) harmonics (3, 5, 7, 9, 11 and 13) decrease almost to zero and the 15th harmonic changes its value.

The phase shift (Fig. 3.1i) decreases to 2 degrees, as expected. Figure 3.1j shows changes in the factor M. Due to a random distribution of active filters powers the factor M increases.

As expected, the optimization resulted in reactive power compensation to the assumed level and minimized the values of the six selected harmonics. A random proportion of the filters contribution to the process of power quality improvement has been chosen randomly, what increased the losses in the system.

The Genetic Algorithm determined the active filters currents; their values are tabulated in Table 3.1.

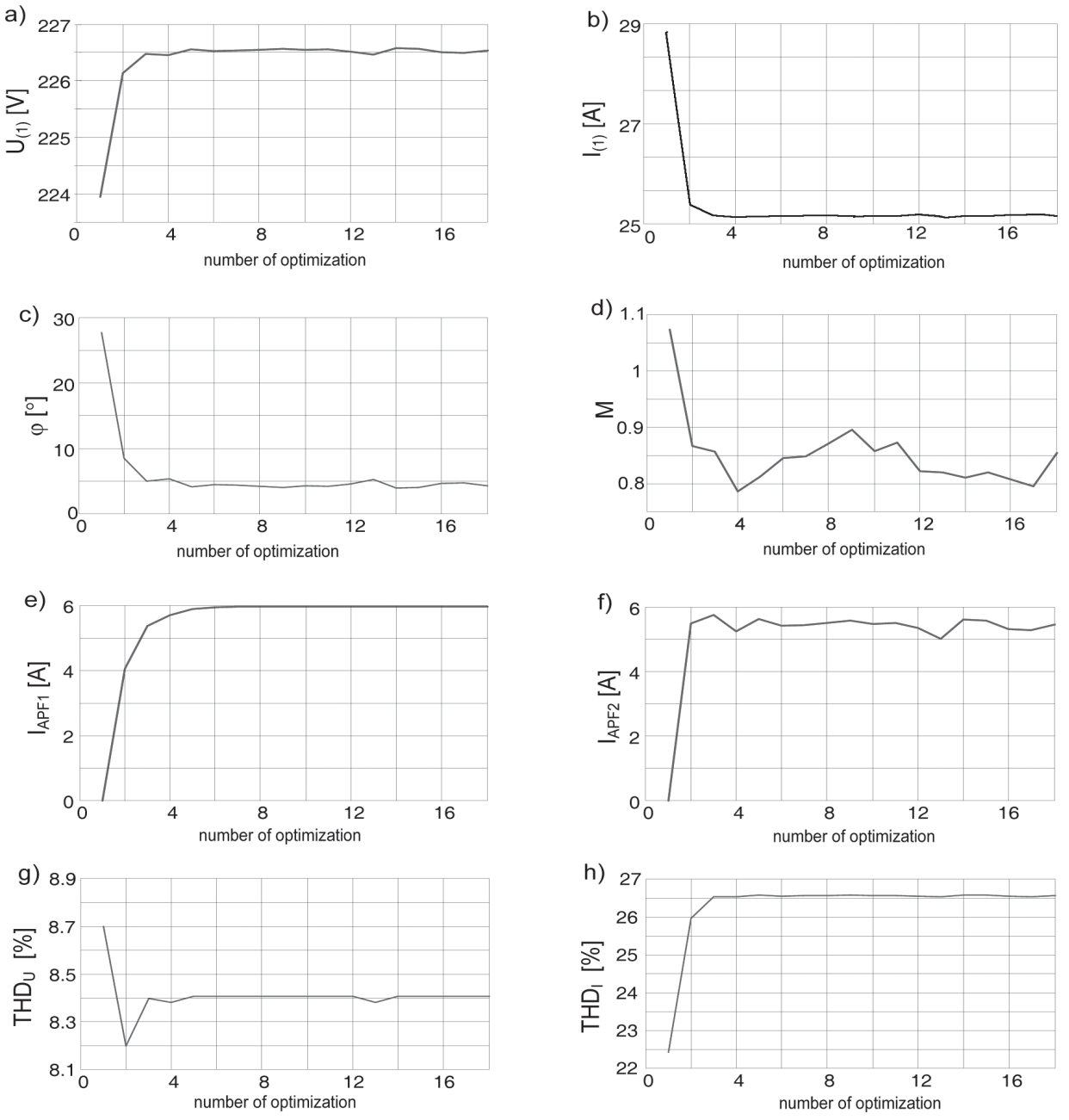

Fig. 2.4. The voltage (a) and current (b) fundamental harmonics; phase shift between the voltage and current fundamental harmonics $\varphi_{(1)}$ (c); the factor M (d); the currents of active filters (e) and (f); distortion factors THD_u (g) and THD_i (h)

3.2. Reduction of the phase shift, harmonics and power losses

The subsequent optimization accounts also for the factor M so as to minimize power losses in the power supply system. The objective function takes the form:

$$f_{goal} = \begin{cases} 10^{10} \cdot |\varphi - 2| & for \ \ \varphi < 2^\circ \\ \varphi - 2 + 20000 \cdot M & for \ \ \varphi \geq 2^c \end{cases} \quad (3.2a)$$

$$f_{goal} = U_h + 20000 \cdot M \quad (3.2b)$$

The simulation result under the above assumptions is shown in Figure 3.2.

Table 3.1. The complex components of active filters currents Reduction of the phase shift, harmonics and power losses.

n	$I_{Re(FA1)}$	$I_{Im(FA1)}$	$I_{Re(FA2)}$	$I_{Im(FA2)}$
1	0.00	–7.33	0.00	–4.79
3	–2.02	2.07	2.57	2.47
5	–1.35	0.94	1.29	–0.58
7	2.80	0.18	1.88	–0.89
9	–0.84	–0.82	0.77	–0.16
11	–0.08	1.75	–0.38	0.49
13	–0.18	–2.21	1.60	–0.40

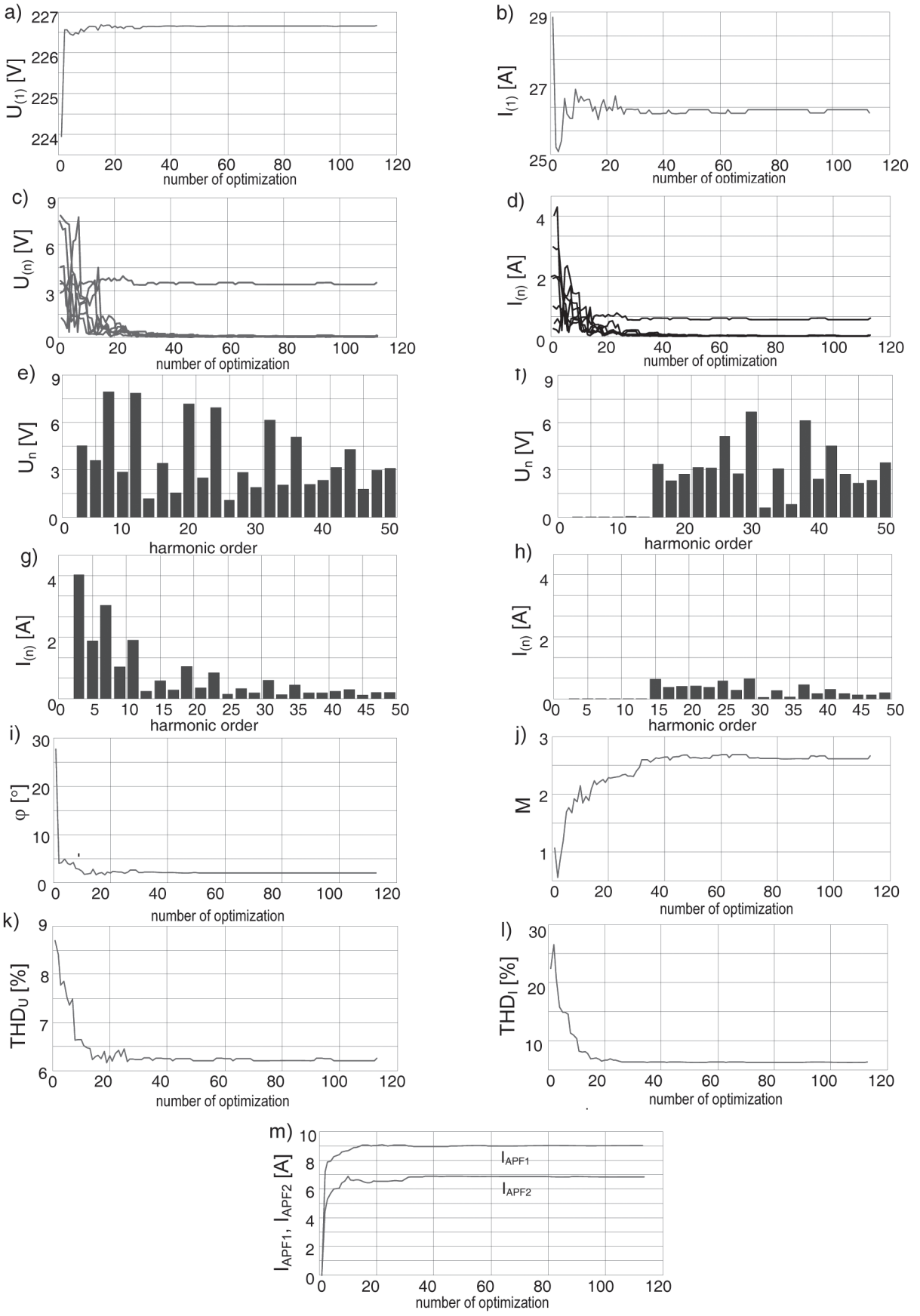

Fig. 3.1. The voltage (a) and current (b) fundamental harmonics; the voltage (c) and current (d) high-order harmonics during the optimization; the voltage spectrum at PCC prior to (e) and after (f) optimization; the current spectrum at PCC prior to (g) after (h) optimization; phase shift (i); the factor M (j); distortion factors THD_u (k) and THD_i (l); active filters currents (m) during the optimization

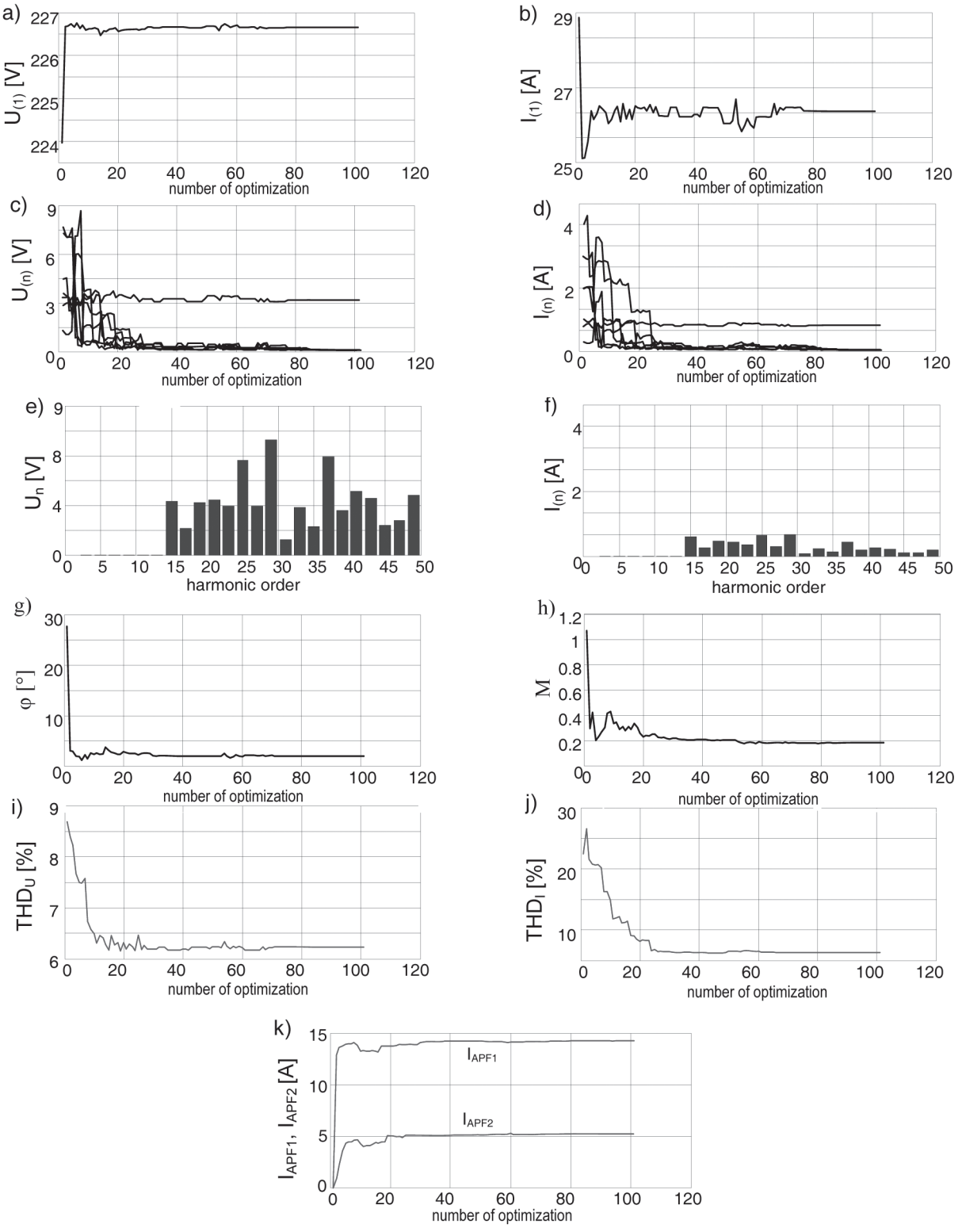

Fig. 3.2. The voltage (a) and current (b) fundamental harmonics; the voltage (c) and current (d) high-order harmonics during the optimization; the voltage (e) and current (f) spectra after optimization; phase shift (g) between the voltage and current fundamental harmonics; the factor M (h); distortion factors THD_u (i) and THD_i (j); active filters currents (k)

The voltage and current harmonics values during the optimization are shown in Figures 3.2a—3.2d. The graphs show amplitudes of the voltage harmonics (3.2c) and current harmonics (3.2d), which were minimized (3, 5, 7, 9, 11 and 13). These harmonics are decreasing almost to zero, though much slower than in the previous case (the Genetic Algorithm randomness should be kept in mind). The voltage and current 15th harmonic, which were not optimized, is also shown in the same graphs. Its value, similarly to other harmonics, is changing during the optimization. It is interesting that values of some, not optimized, high-order harmonics are higher after the optimization then before it. It can be clearly noted in the voltage (3.2e) and current (3.2f) spectra after optimization.

The graph 3.2h shows a change in the factor M. In this case the factor M decreases because the Genetic Algorithm optimized also powers of both active filters. The currents of active filters are shown in Figure 3.2k.

As expected, the optimization resulted in reactive power compensation in the system to the assumed level and reduction of the six selected harmonics values. However, unlikely to the previous optimization, the proportion of active filters currents has been chosen closer to expectation so as the system losses were reduced.

The active filters currents are given in Table 3.2.

3.3. Reduction of the phase shift, harmonics, power losses and operating costs

The subsequent optimization accounts not only for the factor M but also for operating costs of active filters, described by relation (2.4).

The objective function is formulated as:

$$f_{goal} = \begin{cases} 10^{10} \cdot |\varphi - 2| & for \ \ \varphi < 2^\circ \\ \varphi - 2 + 20000 \cdot M + K & for \ \ \varphi \geq 2^\circ \end{cases} \quad (3.3a)$$

$$f_{goal} = U_h + 20000 \cdot M + K \quad (3.3b)$$

The simulation results for the above assumptions are shown in Figure 3.3.

Figure 3.3 shows the voltage (c) and current (d) harmonics values, which were minimized (3, 5, 7, 9, 11 and 13). These harmonics are decreasing almost to zero. It should be noted that during the search for optimum control some harmonics, e.g. the 13th harmonic, may reach much higher values than their initial ones. The 15th harmonic of voltage (c) and current (d), which were not minimized by the Genetic Algorithm also changes its value, reaching values higher then its initial one.

The graph 3.3h shows changes in the factor M. The factor M is reduced but to a lesser extent than in the former example. The currents of active filters are shown in Figure 3.3k.

As expected, the optimization resulted in reactive power compensation in the system to the assumed level, and the values of the six selected harmonics were reduced. With the active filters operating costs taken into account the proportion between their currents has changed. The first filter current has increased while the second filter current decreased. Moreover, it can be noticed a possibility of significant increase in some harmonics above their initial values, both: those being optimized, as well as not optimized.

The active filters currents are given in Table 3.3.

3.4. Reduction of the phase shift, harmonics, power losses and operating costs with limitation of the filter maximum current.

The last optimization takes into account the factor M, operating costs of active filters and limitation of the first filter maximum current. The operating costs (2.4) and the formula of the objective function (3.3a, 3.3b) remain unchanged.

The simulation result under the above assumptions is shown in Figure 3.4.

Figure 3.4 shows the voltage (c) and current (d) harmonics values, which were minimized (3, 5, 7, 9, 11 and 13). These harmonics are decreasing almost to zero however to a lesser extent than in former optimizations. It should be again noted that during the Genetic Algorithm execution some harmonics, before they are reduced, are reaching much higher values than their initial ones, like e.g. the 13th harmonic. The voltage (3.4c) and current (3.4d) 15th harmonic, which were not optimized, is changing during the optimization and also takes values higher then its initial value. The voltage and current spectra after optimization are shown in Figures 3.4e-3.4f. Particularly noticeable are bars of the optimized harmonics because their values after the optimization are higher than prior to it.

The graph in Figure 3.4g shows the phase shift between the voltage and current fundamental harmonics during the optimization. The phase shift has decrease to a value between 2° and 3.5°. It does not stabilize but varies within this range. The graph in Figure 3.4h shows changes in the factor M. In this case the factor M grows from 1.07 to 1.358 what means the increase of 27% of its initial value. The increase is caused by the first active filter current limitation. The necessary

Table 3.2. The complex components of active filters currents

n	$I_{Re(FA1)}$	$I_{Im(FA1)}$	$I_{Re(FA2)}$	$I_{Im(FA2)}$
1	0.00	–12.91	0.00	0.89
3	0.80	4.40	–3.31	0.15
5	2.77	–1.02	–2.97	1.06
7	1.54	0.32	3.35	0.69
9	0.82	–0.64	0.81	0.35
11	0.18	1.18	–1.07	0.83
13	1.55	–1.21	0.30	1.29

Table 3.3. The complex components of active filters currents

n	$I_{Re(FA1)}$	$I_{Im(FA1)}$	$I_{Re(FA2)}$	$I_{Im(FA2)}$
1	0.00	–8.30	0.00	–3.71
3	0.41	4.03	–0.04	0.48
5	3.30	–0.27	–3.48	0.40
7	1.89	0.16	2.97	–0.63
9	0.44	–0.71	–0.46	–0.27
11	–0.26	0.79	–0.60	1.31
13	1.50	–1.06	0.30	–1.51

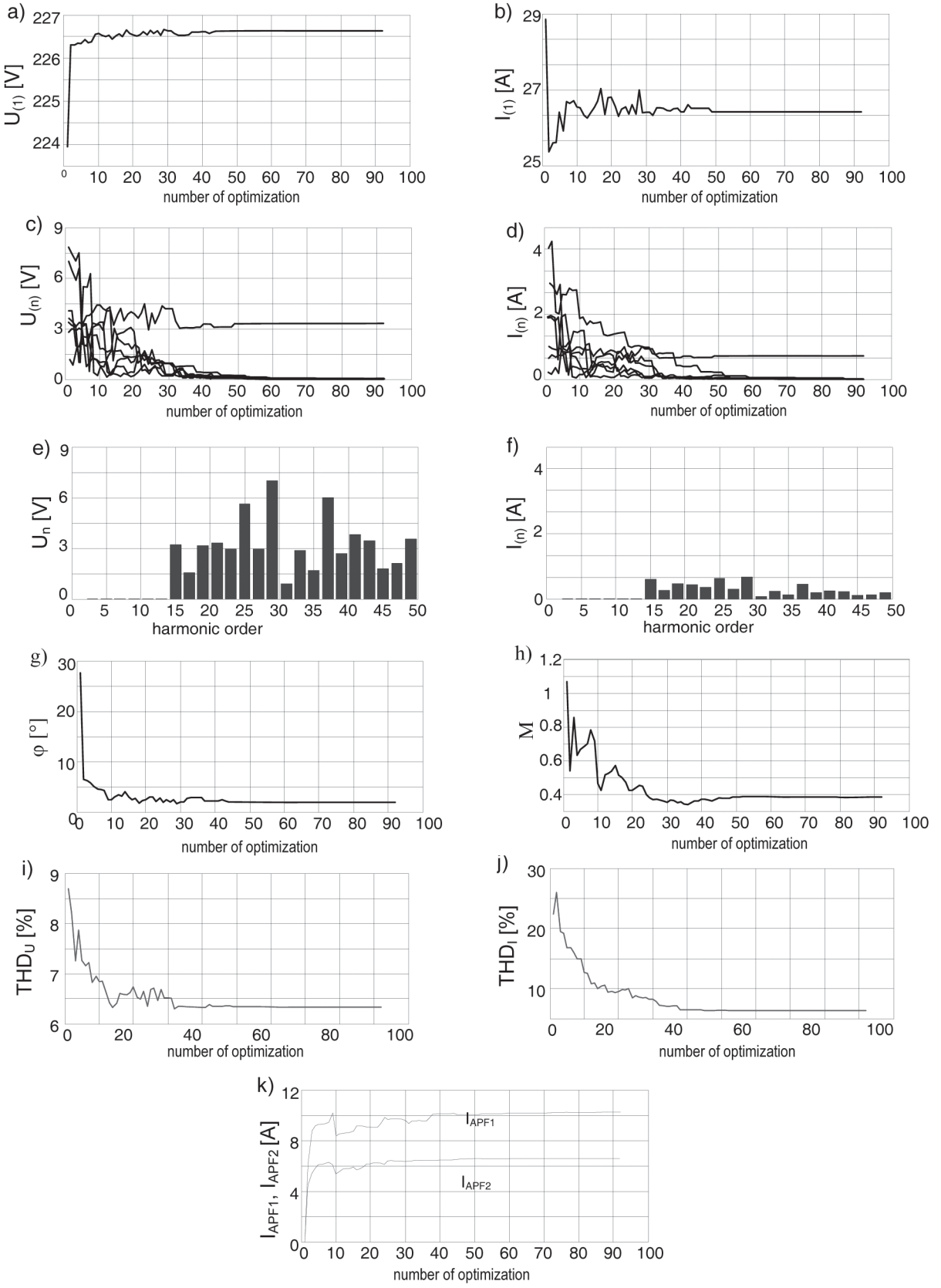

Fig. 3.3. The voltage (a) and current (b) fundamental harmonics; the voltage (c) and current (d) high-order harmonics; the voltage (e) and current (f) spectra after optimization; phase shift (g) between the voltage and current fundamental harmonics; the factor M (h); distortion factors THDu (i) and THDi (j); active filters currents (k)

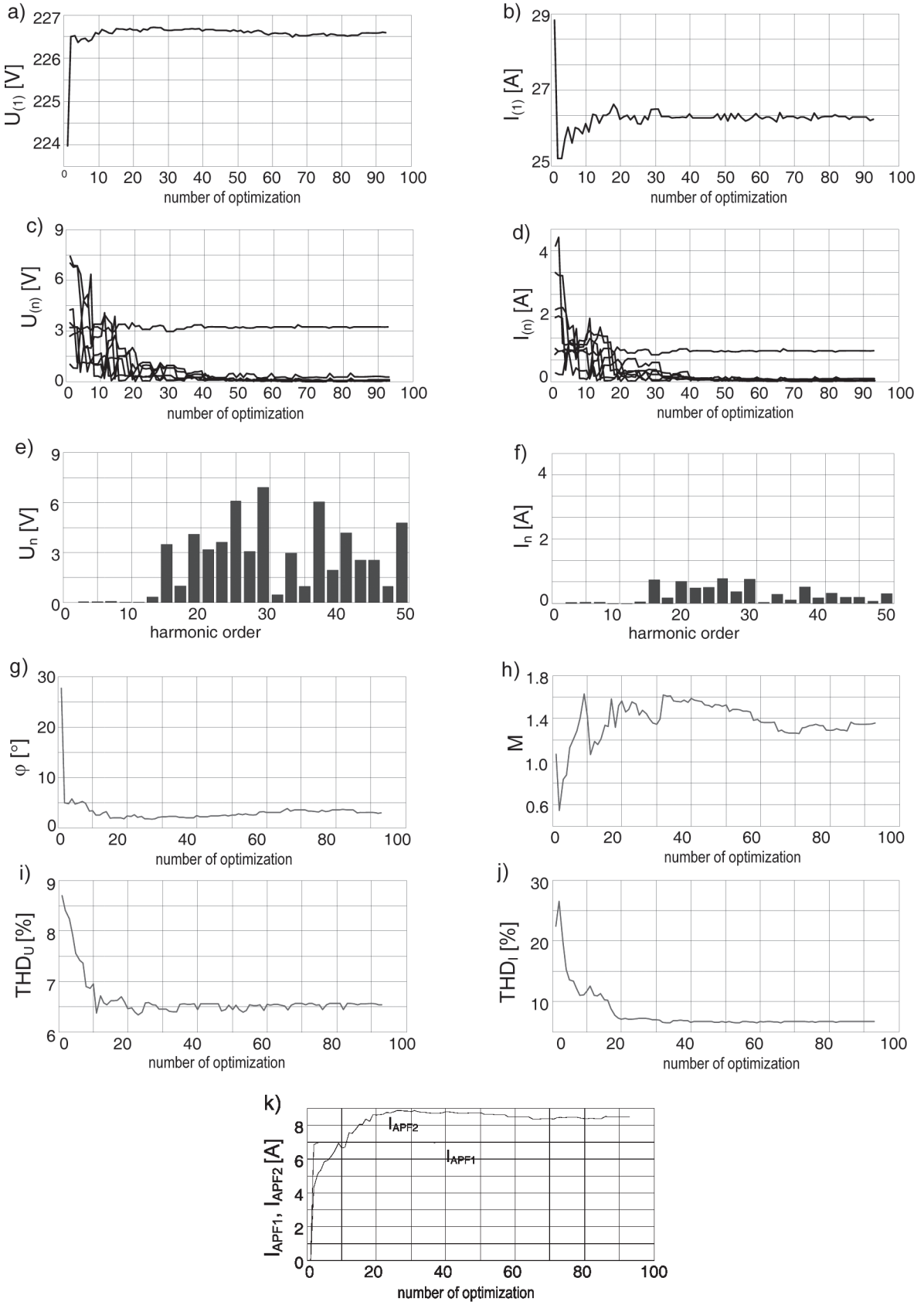

Fig. 3.4. The voltage (a) and current (b) fundamental harmonics; the voltage (c) and current (d) high-order harmonics; the voltage (e) and current (f) spectra after optimization; phase shift (g) between the voltage and current fundamental harmonics; the factor M (h); distortion factors THD_u (i) and THD_i (j); active filters currents (k)

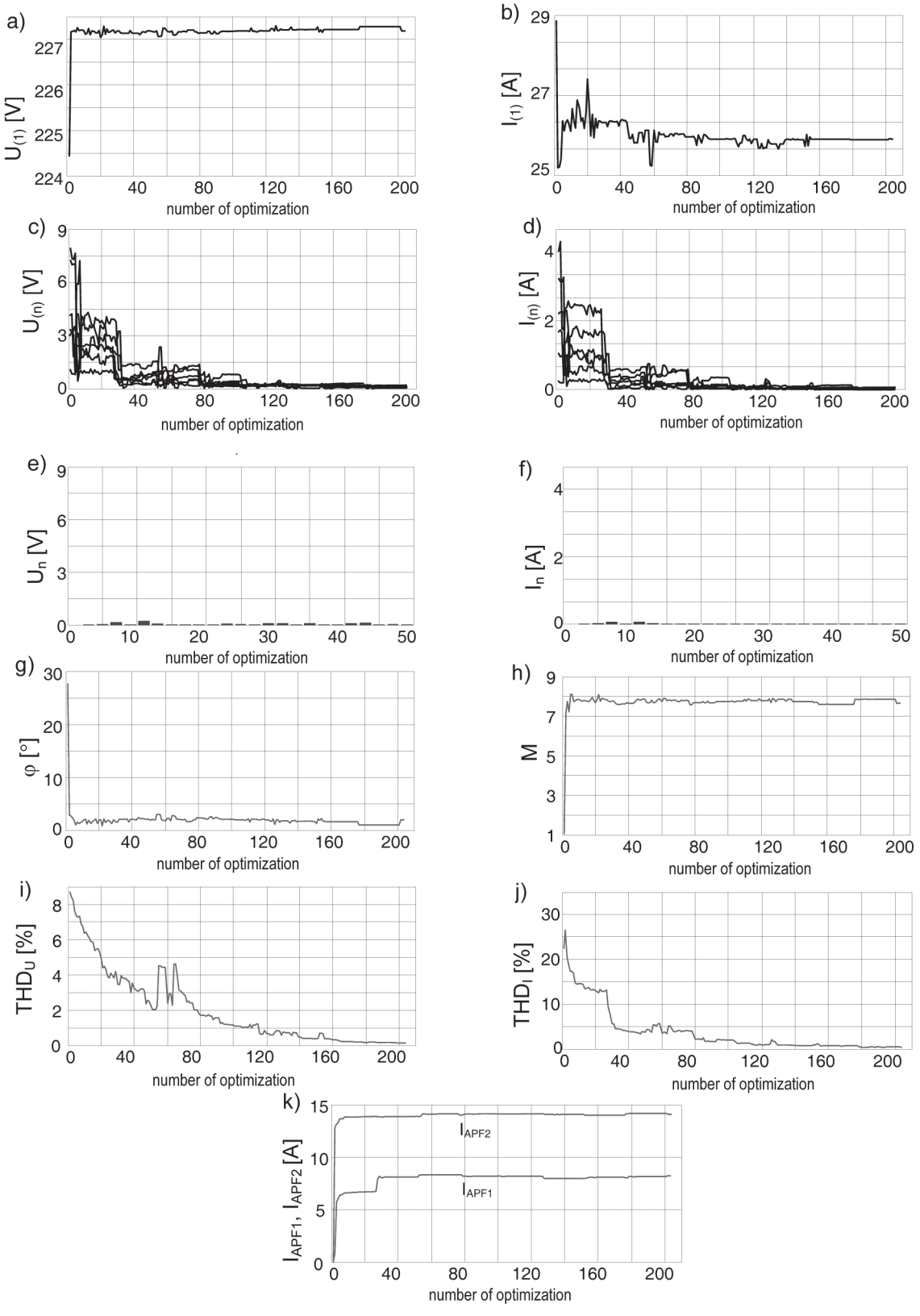

Fig. 4.1. The voltage (a) and current (b) fundamental harmonics; the voltage (c) and current (d) high-order harmonics; the voltage (e) and current (f) spectra after optimization; phase shift (g) between the voltage and current fundamental harmonics; the factor M (h); distortion factors THD_u (i) and THD_i (j); active filters currents (k)

current components are generated by the second filter, more distant from PCC. The currents of active filters are shown in Figure 3.4k.

As expected, the optimization resulted in reactive power compensation in the system, however the assumed level of 2° has not been reached due to a compromise between the power quality and energy cost. With limitation of the first filter current the remaining portion of power is supplied by the second filter, thus causing an increase in the filters' operating costs and losses in the system. Moreover, can be noticed significant increase in some harmonics above their initial values, both: those being optimized, as well as not optimized. The harmonics values undergo strong variations during the optimization. Optimization of one harmonic may result in worsening (i.e. an increase) of other harmonics.

The active filters currents are given in Table 3.4.

4. REACTIVE POWER COMPENSATION WITH SIMULTANEOUS REDUCTION OF 50 HARMONICS

In the two former subsections has been demonstrated that Genetic Algorithms can be successfully applied to optimization of central control of the distributed system for electric power quality improvement. This subsection presents the example of the fundamental harmonic reactive power compensation with simultaneous reduction of all high-order odd harmonics up to the 50th harmonic, with imposed filters operating costs and the first filter current limit of 8A. The active filters operating costs remain as in former examples (2.4). The objective function has not been modified (3.3a, 3.3b).

The simulation results under the above assumptions are shown in Figure 4.1.

The optimization resulted in reactive power compensation in the system. With the first filter maximum current limitation taken into account, the second filter (more distant from PCC) contribution to the task of power quality improvement has increased, thus causing an increase in the filters' operating costs and losses in the system. Moreover, in some harmonics a significant increase above their initial value can be noticed. The harmonics values undergo strong variations during the optimization. Optimization of one harmonic causes changes in the other harmonics, including those already optimized. The explanation of such behavior of the system can be found in changes of the loads operating points.

Table 3.4. The complex components of active filters currents

n	$I_{Re(FA1)}$	$I_{Im(FA1)}$	$I_{Re(FA2)}$	$I_{Im(FA2)}$
1	0.00	–6.84	0.00	–4.45
3	0.28	1.36	0.28	3.19
5	0.73	0.23	–1.13	–0.30
7	0.09	0.11	4.99	–0.67
9	–0.02	–0.05	–0.15	–0.85
11	–0.01	–0.03	–0.77	2.06
13	0,10	–0.10	1.45	–2.54

The components of active filters currents are given in Table 4.1.

5. CONCLUSION

On the basis of the above simulations it can be stated that Genetic Algorithm is a suitable tool for optimizing the control of the distributed system for power quality improvement. It can also be concluded that active filters control can be designed to ensure reactive power compensation in a power system and reduction of selected harmonics up to order of 50. It should be however remembered that the optimization time increases significantly with the number of harmonics due to a number of time-consuming simulations of the system operation, needed by the Genetic Algorithm.

On the basis of the carried out simulations the following conclusions can be drawn:

a) The voltage fundamental harmonic increases and the current fundamental harmonic decreases during the optimization.
b) The phase shift between the voltage and current fundamental harmonics is reduced to the expected value.
c) The factor M value, which represents losses at selected points of the system, has a decisive influence on the current distribution between the filters.

Table 4.1. The complex components of active filters currents

n	$I_{Re(FA1)}$	$I_{Im(FA1)}$	$I_{Re(FA2)}$	$I_{Im(FA2)}$
1	0.00	0.82	0.00	-12.70
3	2.15	6.53	-1.38	-2.02
5	2.57	0.23	-3.08	-0.55
7	1.38	0.46	3.83	-0.55
9	-0.55	-0.78	0.18	-0.09
11	0.41	1.22	-0.79	0.47
13	0.80	-0.77	0.43	-1.54
15	-0.18	0.04	0.63	0.48
17	-0.50	-0.35	0.74	0.21
19	0.35	-0.65	-0.35	-0.06
21	0.06	-0.55	-0.36	0.31
23	0.38	-0.23	0.87	0.06
25	-0.23	-0.12	-0.82	-0.35
27	0.12	0.01	0.26	0.07
29	-0.13	-0.45	0.03	-0.26
31	-0.04	-0.03	0.12	0.06
33	-0.28	0.16	0.02	-0.22
35	0.02	-0.41	-0.17	-0.06
37	-0.36	0.01	0.21	0.01
39	-0.09	-0.19	0.32	0.09
41	-0.04	0.10	-0.65	-0.26
43	-0.01	0.18	0.13	-0.27
45	-0.16	0.09	-0.03	-0.04
47	-0.15	-0.12	0.10	-0.09
49	0.11	0.24	-0.52	-0.04

d) Taking into account operating costs of active filters and their maximum currents worsens the factor M value.
e) In the example system the first active filter has a stronger influence on both: the reactive power compensation and high-order harmonics minimization, than the second active filter.
e) The role of the second active filter becomes more significant after taking into account the operating cost of active filters and limiting the first filter maximum current.
f) The discussed optimizations caused reduction of THD_u and THDi factors due to both: the reduction of selected harmonic values and the increase in the voltage fundamental harmonic.
g) The optimization time depends strongly on the number of optimized harmonics.

Optimization of a selected harmonic causes changes in the adjacent harmonics whose values may increase above their initial value. The same applies to harmonics being reduced.

References

1. Arabas J.: *Lectures of Genetic Algorithms* (in polish). Wydawnictwa Naukowo-Techniczne, Warszawa 2001.
2. Arrillaga J., Bradley D.A., Bodger P.S.: Power System harmonics. John Wiley & Sons, 1985.
3. Cytowski J.: *Genetic Algorithms. Basis and using* (in polish). Akademicka Oficyna Wydawnicza PLJ, Warszawa 1996.
4. El-Habrouk M., Darwish M.K.: *A new control technique for active power filters using a combined genetic algorithm/conventional analysis*. IEEE Trans. on Industrial Electronics, vol. 49, no 1, Feb. 2002.
5. Goldberg D.E.: *Algorithms in Search, Optimization and Machine Learning* (in polish).Wydawnictwa Naukowo-Techniczne, Warszawa 1995.
6. Hanzelka Z., Klempka R.: *Distributed System of Power Quality Improvement*. 19th International Conference on Electricity Distribution, CIRED 2007, Wiedeń 2007.
7. Hartman M., Hashad M., Mindykowski J., Hanzelka Z., Klempka R.: *A new concept of the electrical distributed system for power quality improvement*. 4th International Workshop – Compatibility in Power Electronics, CPE 2005 Gdańsk 2005.
8. Klempka R., Tondos M.: *Application of Genetic Algorithms to improve the power quality in distributed system*. 9th International Conference on Electrical Power Quality and Utilisation, EPQU'07, Barcelona 2007.
9. Klempka R.: *Distributed System for Electrical Power Quality Improvement*, International School on Nonsinusoidal Currents and Compensation ISNCC 2008, 10-13 June 2008, Łagów, Poland.
11. Klempka R.: *Distributed System for Electrical Power Quality Improvement*, Przegląd Elektrotechniczny 200.
12. Michalewicz Z.: *Algorithms in Search, Optimization and Machine Learning* (in polish). WNT, Warszawa 1996.
13. Rutkowska D., Piliński M., Rutkowski L.: *Neural Nets, Genetic Algorithms and Fuzzy logic* (in polish). Wydawnictwo Naukowe PWN Warszawa-Łódź 1997.

14. Rutkowski L.: *Methods and technique of artificial intelligence* (in polish). Wydawnictwo Naukowe PWN, Warszawa 2005.
15. Tolberg L.M., Qi H., Peng F.Z.: *Scalable multi-agent system for real-time electric power management*. Proceedings of IEEE Power Eng. Society Summer Meeting, Vancouver, BC, 15–19 July 2001. Piscataway: IEEE, 2001. vol. 3, p. 1676–1679.
16. Wakileh G.: Power systems harmonics. Springer, 2001.
17. Weiss G. (editor): *Multiagent systems: a modern approach to distributed artificial intelligence*. Cambridge: MIT Press, 1999.

Ryszard Klempka

Ryszard Klempka received the M.Sc. degree in electrical engineering from AGH University of Science and Technology in Cracow, Poland in 1995 and the Ph.D. degree in electrical engineering from AGH in 1999.
Since 1998 he has been a Researcher at AGH in Cracow. His current research interests include evolutionary computation, and power quality.